Journal of Hydroscience and Hydraulic Engineering
Vol. 22, No.1 May, 2004, 51-61

VELOCITY MEASUREMENTS AROUND NON-SUBMERGED AND SUBMERGED SPUR DYKES BY MEANS OF LARGE-SCALE PARTICLE IMAGE VELOCIMETRY

By

FUJITA Ichiro*, MUTO Yasunori**, SHIMAZU Yoshiro***, TSUBAKI Ryota***
and AYA Shiro****

* Department of Architecture and Civil Engineering, Kobe University, Kobe, Japan
** Ujigawa Hydraulics Laboratory, Disaster Prevention Research Institute, Kyoto University, Kyoto, Japan
*** Graduate School, Kobe University, Kobe, Japan
**** Department of Civil Engineering and Urban Design, Osaka Institute of Technology, Osaka, Japan

SYNOPSIS

Field observations on the surface flow were carried out in a straight reach of the Uji River, Kyoto, Japan. Velocity distributions on the water surface were obtained based on the captured video images by means of the Large-Scale Particle Image Velocimetry (LSPIV) developed by Fujita et al. (3). Flow structures around spur dykes are studied for both non-submerged and submerged cases.

It is clearly seen that, for both cases, the dykes work as an additional roughness. Their effect on channel conveyance capacity is estimated in terms of the effective channel width calculated from the velocity distributions. For the non-submerged case the area enclosed by the spur dykes has little contribution to the channel conveyance capacity. Whereas for the submerged case the streamwise velocity is fairly decelerated on the dykes' side due to the drag effect of the dykes themselves. It is also of interest that the maximum velocity filament appears at a different position as the water depth varies in case of the channel with single-side dykes such as studied here. In addition, large-scale boils shedding from the submerged dykes are clearly observed. Their origin and advection mechanisms are also evaluated from the video image. The time period of boils appearing on the water surface is well related with the time calculated by the mean upward velocity and the water depth on the dyke.

INTRODUCTION

Spur dykes and groynes in rivers are introduced originally for navigation maintenance and bank protection. Studies on dykes and groynes fields have for a long time dealt with their function as flow diversion toward the main flow course, and with their stability subject to local scouring around them (Akikusa et al. (1); Fukuoka et al. (4)). Dykes and groynes at the same time facilitate sediment

deposition in the area enclosed by themselves. Such an area provides a preferable environment for natural lives, mainly by a stable flow condition due to slow velocity, and by the variation of the water depth within it as a result of bed topography change. Recently spur dykes and groynes have been constructed again in many rivers, where they are this time expected to show the environmental function described above. As its environmental function was thought to become more and more important, many studies on dykes and groynes fields were started again. Most of them handled hydrodynamics observed in those fields, such as surface oscillation and exchange process (Kimura et al. (7); Ikeda et al. (6); Nezu et al. (14); Ohmoto & Hirakawa (15); Tominaga & Ijima (17)), and some of them extended bed deformations with laboratory experiments (Fukuoka, et al. (5); Ohmoto et al. (16)). There are also a few observations carried out in real rivers (Matsuoka (8); Muneta et al. (9)). From the other point of view, dykes and groynes will arise distortion of the flow field, which leads to increase channel resistance. Their effects on flow structure and bed deformation vary as the water depth changes. Especially when flooding, 3-D nature of the flow is predominant and bed change will be so drastic. This is a quite important point in designing dykes and groynes. However the relation between the flow and bed, and moreover its variation as the depth changes, have not yet been well explored.

This paper deals with flow structure around spur dykes. Velocity measurements on the water surface were carried out in a straight reach of a real river where four dykes are installed on the one side of the main channel. The measurements were conducted under two depth conditions, i.e. the dykes being non-submerged and submerged. Velocity distributions on the surface flow were obtained by means of the Large-Scale Particle Image Velocimetry (LSPIV). The effect of the dykes on channel conveyance capacity is also evaluated from the obtained velocity distributions.

MEASUREMENTS SET-UP

Measurements were carried out at around 42.8km post of the Uji River, Kyoto, Japan. The measurements section is located within a straight reach of the river and its length is about 150m (see Fig. 1). In this section, there are four spur dykes on the right hand side of the main channel. The dykes are set perpendicular to the river-shore line, and its top length is 10m and the distance of the centre of each dyke in the streamwise direction is 40m (see Fig. 2).

In this paper, the results for two different depth conditions were examined. One was the so-called normal condition in which the dykes were not submerged. The measurements for this condition were performed on July 3, 2002, and the river discharge was ca. $90m^3/s$ and the mean water depth in the measurements section was 3.9m. The other measurements were performed on July 11, 2002, under a flooding condition due to passing of a typhoon, in which the dykes were fully submerged. The river discharge and the mean water depth for this condition were ca.$400m^3/s$ and 6.2m respectively, and the water depth over the dykes was 1.2m. The relation between these water depths and the cross sectional view of the channel is shown schematically in Fig. 3.

The motion of the surface flow was, occasionally being visualised with the aid of tracers, captured by digital video cameras set at 20m, 28m and 40m heights on a meteorological observation tower of Disaster Prevention Research Institute, Kyoto University, which is located 100m north of the

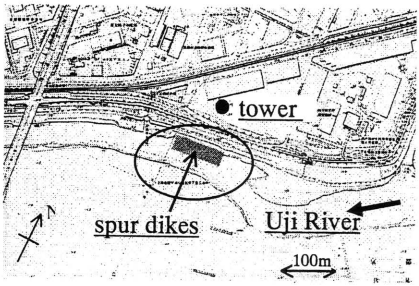

Fig. 1 General view of the observation site (the Uji River;42.5kp~43.3kp)

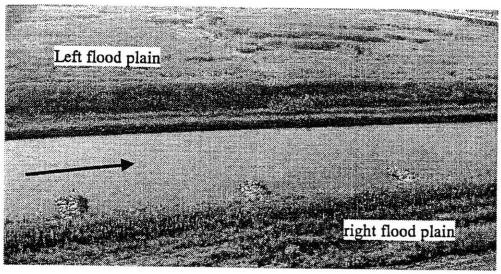

Fig. 2 General view of the observation reach

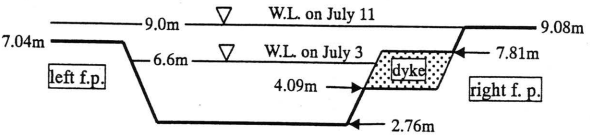

Fig. 3 Schematic view of the relation between water and bed levels

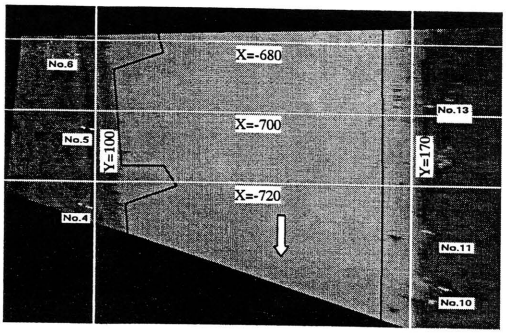

Fig. 4 Definition of coordinates

measurements section. The video images were analysed by means of the Large-Scale Particle Image Velocimetry (LSPIV, Fujita et al. (3)) which yields instantaneous velocity distributions within an area of 60m×60m. 900 images captured with 15Hz were used for the mean flow analyses. Other relevant information as to PIV technique can be found elsewhere in Fujita (2). A definition of the coordinate system in the analyses is shown in Fig. 4. Only the results for the area including the 2nd and 3rd dykes will be shown in the following discussion section.

RESULTS AND DISCUSSIONS

Flow around Dykes

Figure 5 shows velocity distributions for the non-submerged and submerged cases obtained by LSPIV. For the non-submerged case, (a), the main flow region and stagnant area can clearly be recognised. A steep velocity gradient is observed between these areas. The area enclosed by the dykes shows quite small velocities, and such a stagnant area is not within the boundary defined by the tips of dykes, but spreads to a good extent toward the main flow region. In studies of the laboratory experiments, e.g. Muto et al. (12) and Uijttewaal et al. (18), it was reported that there exist one large dominant circulating flow and a few counter cells near the corner in a rectangular embayment. Such an organised motion is, however, not observed here. In contrast, the foregoing measurements carried out by Muto et al. (11) at the same site confirmed the existence of the large circulation flow. After careful observations it was found, apart from the effect of wind, that the circulation flow fluctuates in a rather

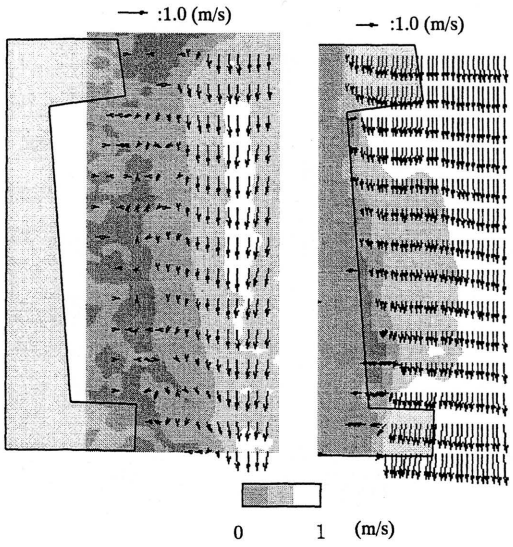

(a) non-submerged (b) submerged

Fig. 5 Velocity distributions around dykes (non-submerged: Y=112 ~ 131m, X=-678 ~ -719m, submerged:Y=100~120m, X=-680 ~ -720m)

long-term duration, over 1 minute, then sometimes being distorted a lot or even disappeared. This may possibly be attributed to the effect of geometry irregularity, but a mechanism producing such a long-term fluctuation is still under investigation.

On the other hand, for the submerged case, (b), almost the whole area runs along the mainstream direction, even in the area enclosed by the dykes. However magnitude of the velocity in that area is smaller, 50 to 60% of that in the main flow region. In addition deceleration rate of the flow is larger as it travels downstream. It is also of interest that the flow over the dykes is, similar to the flow beyond a mound, slightly accelerated due to the smaller water depth on the dykes. These facts support that the existence of the dykes strongly affect velocity distributions around them for the submerged case too. It should be, however, stressed that the internal structure, especially the distorted local flow in the vicinity of the dykes, cannot be detected in the results shown here because they were drawn from the surface flow behaviour only. A further study toward enabling to illustrate the internal 3-D flow structure only with the surface flow behaviour has been started.

Boils for the Submerged Case

When the dykes are submerged, it is deemed that vortex shedding from the dykes and related vertical motion is one of the key issues determining the flow structure. Such an internal structure is, however, not directly detected in this study, because, as shown in the previous chapter, the measurements were only applied to the water surface. Nonetheless, here we paid attention to large-scale boils which were seen quite stably around the dykes. Figure 6 shows the origin and

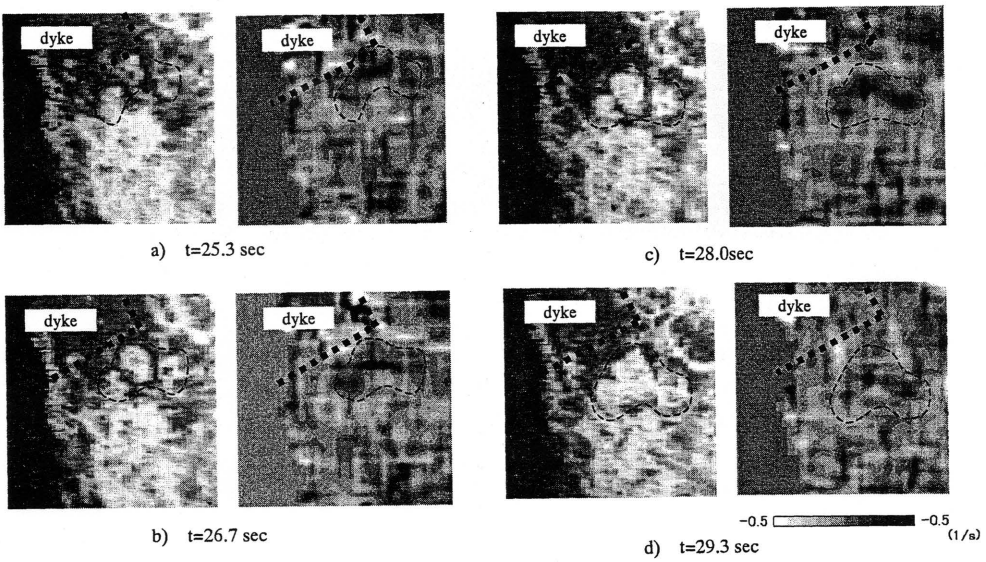

Fig. 6 Advection process of large-scale boils (left:enhanced images, right: divergence distributions; Y=100 ~ 120m,X=-680 ~ -700m)

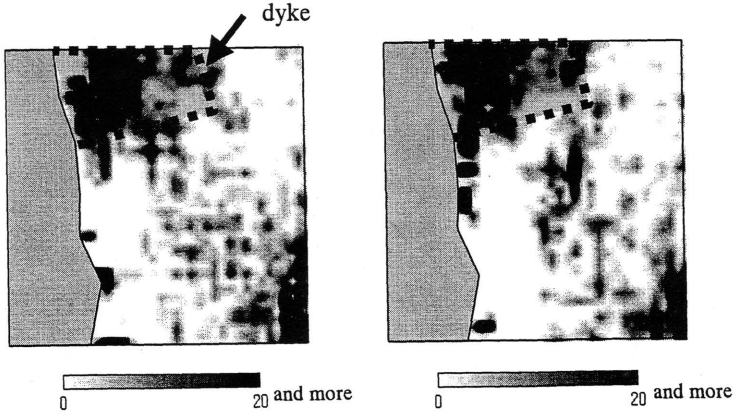

(a) for negative divergence (b) for positive divergence

Fig. 7 Spatial histograms of divergences (threshold level=±0.5(1/s), area same as Fig. 6)

advection processes of the boils observed downstream of the dyke. In the figure, the left side of the pictures are video images with enhancing contrast, and the right side pictures are distributions of divergence calculated from the velocity results, $\partial u / \partial x + \partial v / \partial y$. In the enhanced video images an area which is distinguished with much brighter colour from the ambient region can be recognised (indicated with a dashed circle). Together with careful observations in both raw images and enhanced ones, this brighter colour is realised to show the rising of the water surface, and thus is closely related with boils. In the divergence distributions this area is well correlated with positive peaks, which again indicates the existence of boils. The following pictures in the figure show that such boils are advected without

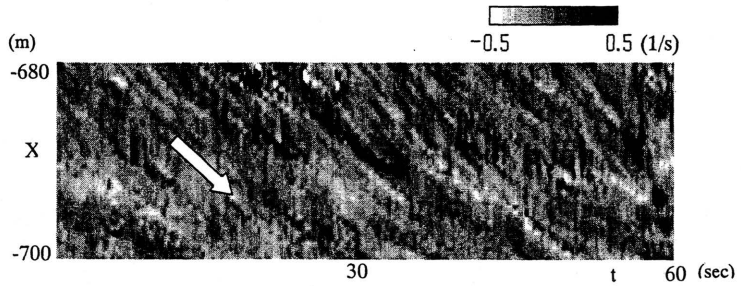

Fig. 8 Space-time image of divergence distribution at Y= 112.25m

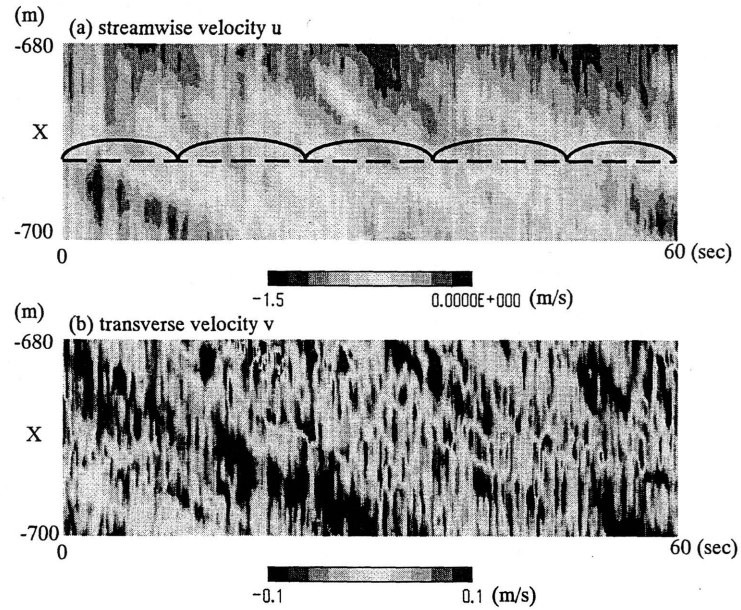

Fig. 9 Space-time image of velocity distributions at Y= 112.25m

changing each of sizes and their mutual distances so much.

Figure 7 shows spatial histograms for both positive and negative divergences in the same area as shown in Fig. 6. In this figure, frequency is counted when the absolute value of divergence exceeds a certain threshold, 0.5 1/s. A distinct area with high frequency can be seen downstream of the tip of the dyke in the figure for positive divergence, (b). At the same area for negative divergence, (a), no such high frequency can be seen. As was shown in Fig. 6 a positive divergence is correlated with a boil, thus this area can be recognised as the point where upward flow reaches the water surface and shows as a boil. From the histogram it can be said that such structure as to the upward flow occurs quite stably and systematically.

Figure 8 shows time variation of the distribution of divergence on a streamwise line including the distinct area considered above. The line is indicated in Fig. 7, Y=112.25m. Figure 8 clearly shows how a boil is advected in time, i.e. one black line indicates origin and advection processes of one boil. Advection velocity can be estimated with the gradient of the line, and is about 1.2m/s, which is nearly the same as the mean velocity of the main flow. In addition, distance of the lines along the time axis

gives period of boil's occurrence, and is about 3.3 seconds. Nezu & Nakagawa (13) summarised that the boil period T can be evaluated as follows: $T^*U_{max}/h=2\sim3$. If the maximum velocity in the main flow and the water depth over the dyke are adopted for U_{max} and h respectively, the above equation yields 2 to 3 seconds for T, which is within the same order with 3.3 seconds through the aforementioned estimation.

Figure 9 shows time variation of the distribution of the streamwise and transverse velocities in the same manner as Fig. 8. It can be seen in the figure that faster flow appears intermittently in a rather long, but nearly fixed, duration (indicated with round lines on a dashed straight line). Judging that this duration is much longer than that of boil examined above, this intermittent faster flow seems to reflect a systematic structure different from boil. The estimated duration from the figure is about 12 seconds, which well coincides with the duration of the first mode of seiche, $2L/\sqrt{gH}$ = 11.5 seconds, assuming that the distance of two dykes, 40m, and the depth in the enclosed area, 4.9m, are adopted for L and H respectively. Surprising is the coincidence of these time scales. Since the submerged flow case is, due to the complexity of the geometry, expected to consist of various time and length scales, it is thought to possess a scale different from the seiche, which is the dominant mechanism for non-submerged cases. Why such extensional use is possible should be further explored in conjunction with close investigation into the internal flow structure. Figure 9 also shows a close correlation between a faster streamwise component and a positive transverse component. Remember that the observed line was on Y=112.25m, i.e. the boundary between the main flow and the dyke-enclosed areas, indicating that the exchange process on the boundary takes place quite systematically.

Channel Conveyance Capacity

Figure 10 shows velocity distributions in the main flow region in a contour form. In the figure velocity is normalised by the maximum velocity of each case. For the non-submerged case, (a), the actual right hand bank is located at Y=110m, nevertheless the normalised velocity becomes almost zero at Y=120m. This means that effective channel width is up to 10m less than the actual one, which is equivalent to about 20% of the channel width. This reduction, 10m, is the same as the top length of the dyke.

Whereas for the submerged case, (b), it should be noted that lateral velocity distribution is asymmetric, i.e. the velocity defect is much smaller on the right side than the left. If the dykes were not installed, its distribution would show the symmetric form from Y=110m and 160m, and the maximum velocity would appear at the centre of the channel, Y=135m. The velocity defect from the normal distribution, as a result of this distortion of the velocity distribution, can be considered as reduction of the effective channel width and yields the defect rate of about 13%.

It is shown that a great deal of channel conveyance capacity is lost due to the existence of the dykes for both non-submerge and submerged cases. For the non-submerged case, this can mainly be attributed to the flow diversion away from the shore, hence a large stagnant area is clearly formed behind a dyke. Whereas for the submerged case, the distortion of the velocity field implies that a dyke plays as an additional roughness element. Thus it can be said that mechanisms bringing the capacity

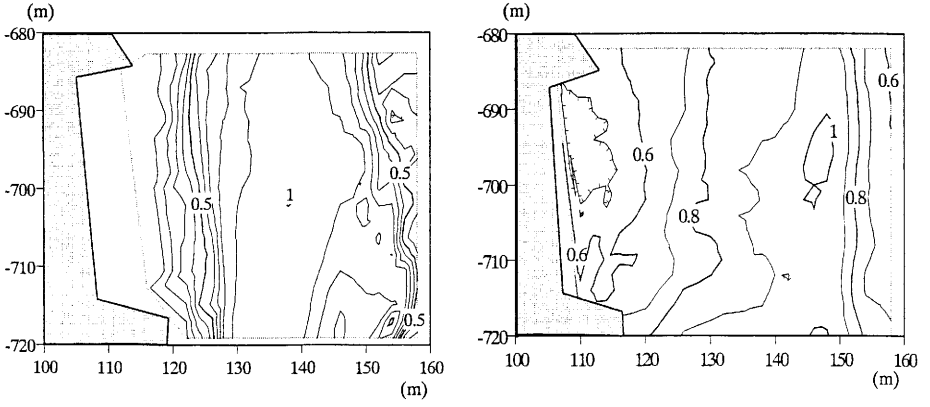

Fig. 10 Streamwise velocity distributions normalized by maximum surface velocity

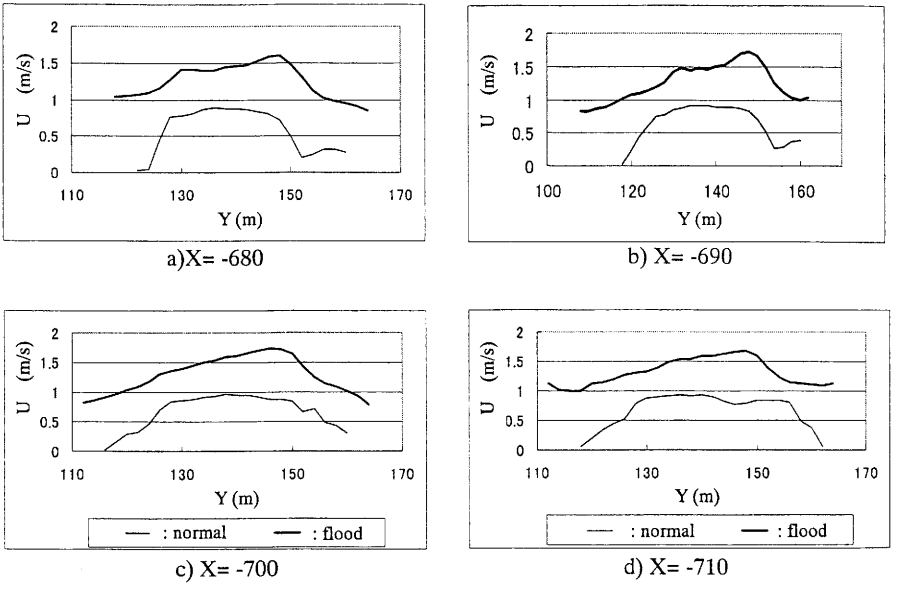

Fig. 11 Comparison of streamwise velocity distributions

reduction differ somewhat with depth conditions.

Maximum Velocity Filament

Figure 11 shows lateral distributions of the streamwise velocity at different locations, X=-680m to –710m. For the non-submerged case the maximum velocity appears at around Y=135 to 140m, which is almost at the centre, or slightly shifted toward the left hand bank, of the channel. For the submerged case, as can be also seen in Fig. 10, the shift of the maximum toward the left hand bank is much remarkable. The maximum velocity appears at around Y=145 to 150m.

The reason for such a shifting according to the depth condition is not clear at the moment, but can be attributed to the river channel geometry preceding the test section. A sand bar existing about

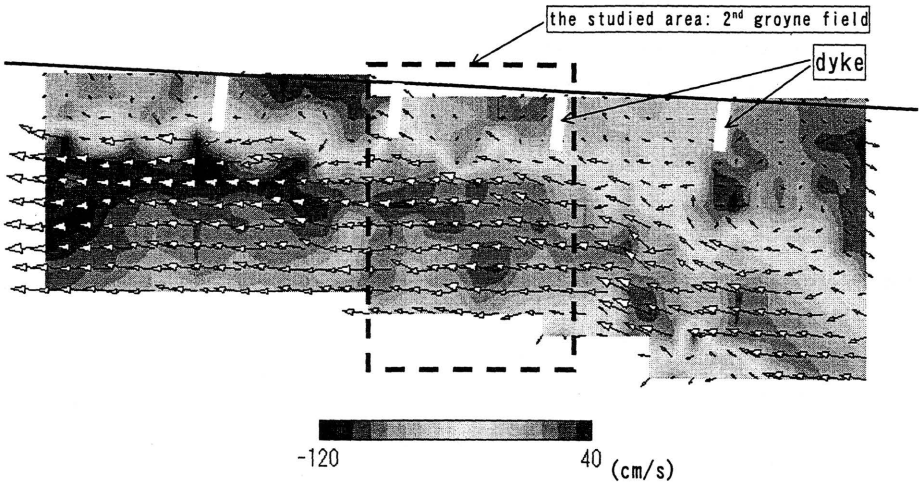

(a) 0.36m below the water surface

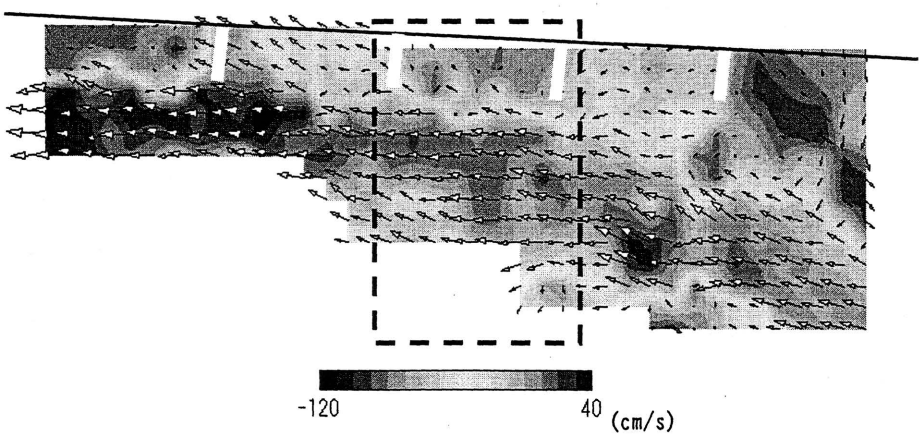

(b) 2.11m below the water surface

Fig. 12 Velocity distributions for the non-submerged case measured by an ADCP

200m upstream on the right shore of the main channel (see Fig. 1) may play an important function for the flow structure in the test section. For example, the effect of this sand bar on the in-flow condition can clearly be seen in Fig. 12. The figure shows the velocity distributions in the water measured by a ship-mounted ADCP for the non-submerged case in a reach of about 200m including the whole groyne fields (the field mainly considered in this paper is indicated with a dashed-line square). Details for the measurements can be found elsewhere in Muto (10). It is noteworthy that, irrespective of the measured depths, a large inverse flow region is formed upstream of the first dyke, or behind the bar in other words, and the main flow seems to take circuitously from the inverse flow region. It should also be noted that this bar disappears under the water when river discharge becomes large, such as the submerged case considered here, which will totally change the in-flow condition.

It should stressed that this variation of appearing the maximum velocity is quite important

when considering river maintenance, since position of the maximum velocity is often related with that of the maximum scouring. Further study has been started in order to draw a relationship between the shifting distance and the water depth under different depth conditions.

CONCLUSIONS

Flow structure around spur dykes is studied in a real river based on the velocity measurements by large-scale particle image velocimetry. When the dykes are not submerged the area enclosed by the dykes is almost stagnant, and channel conveyance capacity is lost in a great deal due to the area. When the dykes are submerged the flow affected by the dykes is decelerated considerably. For the submerged case, in addition, 3-D structure related with a vertical motion is deemed to be more dominant, and boils observed downstream of the dykes can be one of the examples of such a motion. Boils occur quite stably, and their advecting velocity and occurring period is well related with the main flow velocity and the water depth over the dyke. The effect of the dykes on velocity distributions varies as the water depth changes. It is important that the maximum velocity filament appear at a different position when the depth changes in a river with dykes on the one side such as studied here.

ACKNOWLEDGEMENT

The authors would acknowledge Yodogawa Public Works Office, MLIT, Japan, for their support and guidance on the field measurements. The authors would also thank Drs. Takehara, K. (Kinki Univ.), Miyamoto, H. (Kobe Univ.), Tamai, M. (Osaka Univ.) and Takano, Y. (Kinki Univ.) for their comments through discussions.

REFERENCES

1. Akikusa, I, Kikkawa, H, Sakagami, Y, Ashida, K & Tsuchiya, A: A study on the hydraulics of groynes, *Technical Report of PWRI*, MOC, Japan, No.107-6, 1960. (in Japanese)
2. Fujita, I: Video image analysis of inter-groin surface flow by using environment-friendly tracer, *Annual J. Hydr. Eng.*, JSCE, Vol.42, pp.505-510, 1998. (in Japanese)
3. Fujita, I, Muste, M & Kruger, A: Large-scale particle image velocimetry for flow analysis in hydraulic engineering applications, *J. Hydr. Res.*, Vol.36, No.3, pp.397-414, 1998.
4. Fukuoka, S, Watanabe, A & Nishimura, T: On the groin arrangement in meandering rivers, *J. Hydr. Coast. and Environ. Eng., JSCE*, No.443/II-18, pp.27-36, 1992. (in Japanese)
5. Fukuoka, S, Nishimura, T, Okanobu, M & Kawaguchi, H: Flow and bed topography around groins installed in a straight channel, *Annual J. Hydr. Eng.*, JSCE, Vol.42, pp.997-1002, 1998. (in Japanese)
6. Ikeda, S, Yoshiike, T & Sugimoto, T: Experimental study on the structure of open channel flow with impermeable spur dikes, *Annual J. Hydr. Eng.*, JSCE, Vol.43, pp.281-286, 1999. (in Japanese)
7. Kimura, I, Hosoda, T & Muramoto, Y: Characteristics of suspended sediment transport in open channel flows with a dead zone, *Annual J. Hydr. Eng.*, JSCE, Vol.42, pp.1057-1062, 1998. (in

Japanese)

8. Matsuoka, Y: Characteristics of large eddies among groynes, *Annual J. Hydr. Eng.*, JSCE, Vol.39, pp.773-778, 1995. (in Japanese)
9. Muneta, N, Shimizu, Y & Itakura, T: About grain size distribution and river bed change around a spur-dike with a flood, *Annual J. Hydr. Eng.*, JSCE, Vol.40, pp.799-804, 1996. (in Japanese)
10. Muto, Y: ADCP, its application to river flow measurements, *Annuals of Disas. Prev. Res. Inst.*, Kyoto Univ., No.47B, to be submitted, 2004.
11. Muto, Y, Baba, Y & Fujita, I: Velocity measurements in rectangular embayments attached to a straight open channel, *River Flow 2002*, Louvain-la-Neuve, Belgium, pp.1213-1219, 2002.
12. Muto, Y, Imamoto, H & Ishigaki, T: Turbulence characteristics of a shear flow in an embayment attached to a straight open channel, *Advances in Hydro-Science and –Eng.*, Volume IV, p.232, 2000.
13. Nezu, I & Nakagawa, H: *Turbulence in Open-channel Flows*, Balkema, p.217, 1993.
14. Nezu, I, Onitsuka, K and Iketani, K: Measurements of open-channel flows with a horizontally dead zone by using PIV technique, *J. Hydr. Coast. and Environ. Eng., JSCE*, No.677/II-55, pp.53-61, 2001. (in Japanese)
15. Ohmoto, T & Hirakawa, R: Turbulent flow and free-surface oscillation in an open channel with spur dikes, *Annual J. Hydr. Eng.*, JSCE, Vol.46, pp.469-474, 2002. (in Japanese)
16. Ohmoto, T, Hirakawa, R & Ide, K: Responses of secondary currents and sediments to submerged groynes, *Annual J. Hydr. Eng.*, JSCE, Vol.42, pp.1003-1008, 1998. (in Japanese)
17. Tominaga, A & Ijima, K: Effects of interval length on flow structures around submerged spur dikes, *Annual J. Hydr. Eng.*, JSCE, Vol.46, pp.475-480, 2002. (in Japanese)
18. Uijttewaal, WSJ, Lehmann, D & van Mazijk, A: Exchange processes between a river and its groyne fields: Model experiments, *J. Hydr. Engrg.*, Vol.127, No.11, pp.928-936, 2001.

APPENDIX – NOTATION

The following symbpls are used in this paper:

h = the water depth over the dyke;

H = the water depth in the groyne field;

L = the distance of the two successive dykes (= i.e. 40m);

T = the boil period;

U = the time averaged streamwise velocity;

U_{max} = the maximum velocity in the main flow region;

X = the streamwise distance; and

Y = the transverse distance.

(Received July 2, 2003 ; revised October 1, 2003)